

ORIGINAL ARTICLE

Unraveling the Pharmacokinetic Interaction of Ticagrelor and MEDI2452 (Ticagrelor Antidote) by Mathematical Modeling

J Almquist^{1,2,3}, M Penney⁴, S Pehrsson³, A-S Sandinge³, A Janefeldt³, S Maqbool⁴, S Madalli⁵, J Goodman⁴, S Nylander³ and P Gennemark^{3*}

The investigational ticagrelor-neutralizing antibody fragment, MEDI2452, is developed to rapidly and specifically reverse the antiplatelet effects of ticagrelor. However, the dynamic interaction of ticagrelor, the ticagrelor active metabolite (TAM), and MEDI2452, makes pharmacokinetic (PK) analysis nontrivial and mathematical modeling becomes essential to unravel the complex behavior of this system. We propose a mechanistic PK model, including a special observation model for post-sampling equilibration, which is validated and refined using mouse *in vivo* data from four studies of combined ticagrelor-MEDI2452 treatment. Model predictions of free ticagrelor and TAM plasma concentrations are subsequently used to drive a pharmacodynamic (PD) model that successfully describes platelet aggregation data. Furthermore, the model indicates that MEDI2452-bound ticagrelor is primarily eliminated together with MEDI2452 in the kidneys, and not recycled to the plasma, thereby providing a possible scenario for the extrapolation to humans. We anticipate the modeling work to improve PK and PD understanding, experimental design, and translational confidence.

CPT Pharmacometrics Syst. Pharmacol. (2016) 5, 313–323; doi:10.1002/psp4.12089; published online 16 June 2016.

Study Highlights

WHAT IS THE CURRENT KNOWLEDGE ON THE TOPIC?

☑ Antiplatelet therapy for the prevention of atherothrombotic events in patients with acute coronary syndrome is known to increase the risk of bleeding complications. The unique reversible binding mode of action of the oral antiplatelet agent, ticagrelor, has enabled the development of MEDI2452, a ticagrelor-specific antidote for rare emergency situations.

WHAT QUESTION DOES THIS STUDY ADDRESS?

☑ This study seeks to unravel the PK interaction between ticagrelor and MEDI2452 through the use of mathematical modeling, aiming for both qualitative understanding as well as detailed quantitative predictions.

WHAT THIS STUDY ADDS TO OUR KNOWLEDGE

☑ A mathematical model describing the simultaneous PKs of ticagrelor and MEDI2452 in the mouse is presented. The model offers a mechanistic explanation for the complex kinetics and can predict the unobserved free ticagrelor plasma concentration that drives the platelet aggregation PDs.

HOW THIS MIGHT CHANGE DRUG DISCOVERY, DEVELOPMENT, AND/OR THERAPEUTICS

☑ The combined ticagrelor-MEDI2452 model can contribute to the development of MEDI2452 by assisting in interpretation of observed data, by prediction of free ticagrelor and TAM plasma concentrations, and by simulation of experimental designs.

Ticagrelor is a direct acting and reversibly binding P2Y₁₂ antagonist.¹ In the PLATO study, a positive benefit-risk profile for the prevention of atherothrombotic events in patients with acute coronary syndrome was established.² Based on the PLATO data, as well as data with the thienopyridines, clopidogrel in CURE,³ and prasugrel in TRITON,⁴ dual antiplatelet therapy, consisting of aspirin and a P2Y₁₂ antagonist, is critical for the treatment of acute coronary syndrome. In addition, in the recently completed PEGASUS TIMI-54, the benefit-risk profile for long-term treatment with ticagrelor in patients with a history of myocardial infarction and a high risk of developing an atherothrombotic event was documented supporting the

use of ticagrelor for long-term treatment.⁵ However, all antiplatelet therapies are known to increase the risk of bleeding complications.^{2–5} The unique reversibly binding mode of action of ticagrelor provides an opportunity for developing a specific reversal agent not possible for the thienopyridines, which are all irreversible P2Y₁₂ antagonists. The first data for the ticagrelor-specific neutralizing antibody fragment (Fab), MEDI2452, has recently been published.⁶

MEDI2452 specifically binds free (unbound to plasma proteins) ticagrelor and free AR-C124910XX—the ticagrelor active metabolite (TAM)—with a high affinity of about 20 pM.^{6,7} MEDI2452 thereby prevents ticagrelor's and

¹Fraunhofer-Chalmers Centre, Chalmers Science Park, Gothenburg, Sweden; ²Systems and Synthetic Biology, Department of Biology and Biological Engineering, Chalmers University of Technology, Gothenburg, Sweden; ³Cardiovascular and Metabolic Diseases, Innovative Medicines, AstraZeneca R&D, Mölndal, Sweden; ⁴Clinical Pharmacology and DMPK, MedImmune, Cambridge, UK; ⁵Cardiovascular and Metabolic Diseases Research, MedImmune, Cambridge, UK. *Correspondence: P Gennemark (peter.gennemark@astrazeneca.com)

Received 8 February 2016; accepted 4 May 2016; published online 16 June 2016. doi:10.1002/psp4.12089

TAM's (similar potency vs. P2Y₁₂ as ticagrelor) interaction with, and inhibition of, the platelet P2Y₁₂ receptor. MEDI2452 may prove valuable as an agent for patients on ticagrelor therapy who require urgent surgery or suffer an acute major bleed. If successful, MEDI2452 would be the first antidote for an antiplatelet drug. Recently, specific antidotes for oral anticoagulants have been described and are undergoing clinical trials, including a specific Fab for the thrombin inhibitor dabigatran, idarucizumab,^{8–11} and a recombinant catalytically inactive Factor (F)Xa, andexanet alfa, which is targeted to reverse all the FXa inhibitors.¹²

The main objective of the present work is to better understand the pharmacokinetics (PKs) of ticagrelor, TAM, and MEDI2452, in general, and to be able to predict free plasma concentrations of ticagrelor and TAM in particular. Knowledge of free plasma concentrations is crucial as it is only the free fractions—and not the more than 99% protein-bound fraction or the dynamically changing MEDI2452-bound fraction—that can inhibit the P2Y₁₂ receptor and thereby drive the pharmacodynamic (PD) response. The PK analysis is complex because of the dynamic interaction that occurs between these compounds when administered to the same system. It is expected that mathematical modeling will be essential for unraveling their combined PK behavior. In addition, we investigate if a simple turnover model driven by the predicted free levels can describe PD data of platelet aggregation. The work was accomplished in three stages. First, a mathematical model of the combined ticagrelor-MEDI2452 PK in the mouse was set up based on data of separately administered ticagrelor and MEDI2452, and on assumptions supported by literature. Second, the model was validated and refined using several different combined ticagrelor-MEDI2452 PK datasets not used in the first stage. Finally, the model was used to understand how the complex PK emerges from the ticagrelor-MEDI2452 interaction. Specifically, we let the model predict free plasma levels of ticagrelor and TAM under different experimental designs, and, in turn, let these predictions drive the PD model.

MATERIALS AND METHODS

MEDI2452 prestudy: dosing only MEDI2452 to rats

MEDI2452 PK was observed following a 1,000 mg × kg⁻¹ i.v. bolus dose in conscious Sprague-Dawley rats. Venous serum samples were obtained predose and at 5, 15, and 30 minutes, and 1, 2, 6, 12, 24, and 48 hours postdose. The study was performed by Huntingdon Life Sciences (Huntingdon, UK) in compliance with the United Kingdom Animals (Scientific Procedures) Act 1986 Amendment Regulations 2012.

Ticagrelor prestudies: dosing only ticagrelor to mice

Ticagrelor PK in nonfasted male C57Bl6 mice (Charles River, Sulzfeld, Germany; body weight in the range of 15–25 g) was observed in two studies, of which the first also included TAM observations. The studies were approved by the ethical committee for animal research at the University of Göteborg, Sweden. Mice were anesthetized with isoflurane vapor (Forene; Abbot Scandinavia AB, Sweden). A catheter was inserted in the left jugular vein for administration of the vehicle or drug. The body temperature was maintained at 38°C by external heating. In the first study, four mice were given ticagrelor as an

i.v. infusion at a rate of 240 μg × min⁻¹ × kg⁻¹ for 5 minutes, followed by 30 μg × min⁻¹ × kg⁻¹ for 15 minutes. The ticagrelor and TAM total concentrations (free and protein-bound) in plasma were observed at 20, 30, 40, 50, 65, and 80 minutes after the start of infusion (thus, the first sample was collected immediately poststop of infusion). In the second study, two mice were administered an i.v. bolus dose of 2,000 μg × kg⁻¹ ticagrelor. The total ticagrelor concentration in blood was measured in samples collected at 2, 5, 10, 30, 60, 90, 120, and 150 minutes after the dose.

Main studies: dosing MEDI2452 to ticagrelor-treated mice

Four different studies in nonfasted male C57Bl6 mice were used for model validation and refinement, labeled study 1 to 4. Their designs are illustrated in **Figure 1**, and the full details are given in **Supplementary Text S1**. Animal handling and experimental setup were as described for the ticagrelor pre-studies. In common with these studies, the mice were first dosed with an i.v. infusion of ticagrelor, allowing the plasma concentration to reach steady-state. Then, a bolus of the antidote MEDI2452 was administered. The PD data from studies 1, 3, and 4 have previously been reported.⁶

Bioanalysis

Quantification of total (free and protein bound) as well as free (protein unbound) ticagrelor and TAM in plasma samples in the mouse was determined by protein precipitation and liquid chromatography mass spectrometry. The lower limits of quantification of free ticagrelor and TAM were 0.03 nmol L⁻¹ and 0.06 nmol L⁻¹. Quantification of MEDI2452 in mouse and rat plasma was performed with the Gyrolab nanoliter scale immunoassay assay platform. Mouse and rat assays had lower limits of quantification of 260 and 350 ng × mL⁻¹. Quantification of ADP-induced platelet aggregation was evaluated using the Multiplate impedance aggregometer (Dynabyte, Munich, Germany). Further details of the bioanalysis are given in **Supplementary Text S1**.

Data analysis

Parameter estimation was performed according to a maximum likelihood approach with a multiplicative lognormal error model for the PK model and a mixed additive and multiplicative error model for the PD model, using the naive-pooled data approach. Uncertainty of parameter estimates was determined by bootstrapping, sampling single measurements randomly with replacement within each experiment ($N = 300$). Uncertainty of the final PK model used for predictions and for driving the PD model was generated based on Monte Carlo sampling from the parameter distributions obtained from bootstrapping, and from additional parameter uncertainties defined in **Table 1**. In addition to uncertainty with respect to parameter values, model predictions also incorporate the effect of uncertainty resulting from the model's residual variability (**Supplementary Text S2**).

Numeric analyses were performed in MATLAB (R2014a; The MathWorks, Natick, MA). Specifically, the Matlab function *fminsearch* was used for solving the optimization problems encountered during parameter estimation. The Matlab model code is provided in the **Supplementary Model Code files**. The analytical solution used in the observation model was derived in Mathematica 10 (Wolfram Research, Champaign, IL).

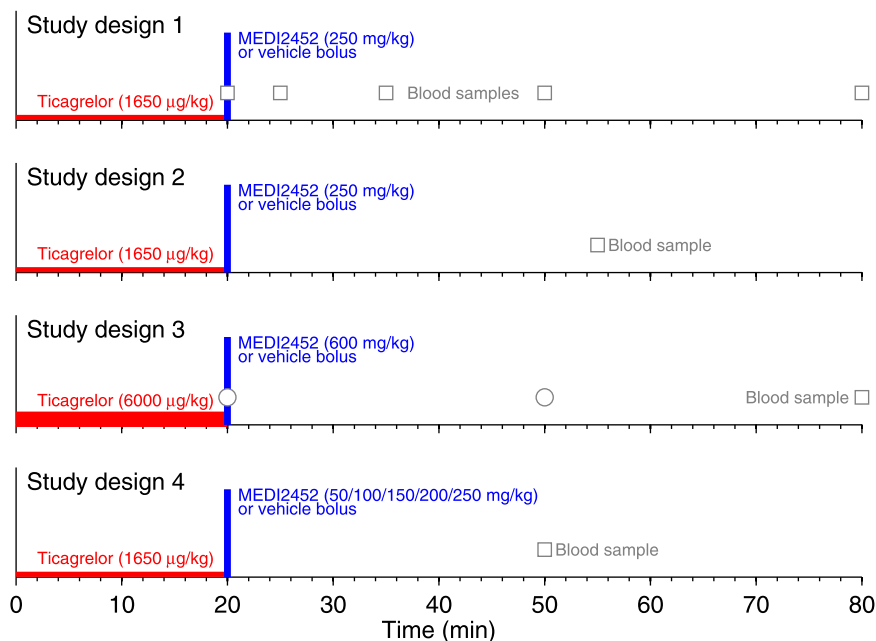


Figure 1 Designs of validation studies 1 to 4. Mice were given ticagrelor as an i.v. infusion during 20 minutes. Immediately after the ticagrelor infusion, an i.v. bolus dose of MEDI2452 or vehicle was given. Terminal blood samples for plasma exposure of ticagrelor and MEDI2452 were collected at various time-points. For study design 3, gray circles indicate blood samples from a separate pharmacokinetic experiment.

RESULTS

PK models for only ticagrelor or MEDI2452

Before the combined ticagrelor-MEDI2452 interaction model could be set up, two independent PK models were derived for the separate administration of ticagrelor in the mouse

and of MEDI2452 in the rat. The details of these models are described in **Supplementary Text S2**, **Supplementary Figure S1**, and **Supplementary Figure S2**. We found that ticagrelor (and TAM) follows two-compartment kinetics in the absence of MEDI2452, and that MEDI2452 kinetics in

Table 1 Model parameters

Name	Unit	Value	Estimated value	Uncertainty	Explanation
f	–	0.0020	0.0020 (not estimated)	0.0012, 0.0028 ^a	Fraction unbound ticagrelor (internal data, $n = 38$)
k_{on}	$\text{nM}^{-1} \times \text{min}^{-1}$	0.14	0.11	0.078, 0.122 ^b	Second-order rate constant. Initial point estimate obtained from different estimates of the rate constants of the similarly sized ligands methotrexate, dabigatran, and toptotecan. ^{8,17,20,27}
K_d	nM	0.02	0.02 (not estimated)	0.013, 0.029 ^c	Affinity of MEDI2452 for ticagrelor and TAM. ⁶
Cl_{met}	$\text{L} \times \text{min}^{-1} \times \text{kg}^{-1}$	0.012	0.0080	0.0077, 0.0083 ^b	TAM-specific ticagrelor clearance
Cl	$\text{L} \times \text{min}^{-1} \times \text{kg}^{-1}$	0.058	0.022	0.019, 0.025 ^b	Remaining ticagrelor clearance
V_1	$\text{L} \times \text{kg}^{-1}$	1.63	1.12	0.95, 1.18 ^b	Initial estimate obtained by $V_{1,Tica} - V_{MEDI2452} = 1.68 - 0.05 \text{ L} \times \text{kg}^{-1}$
Cl_d	$\text{L} \times \text{min}^{-1} \times \text{kg}^{-1}$	0.042	0.041	0.050, 0.066 ^b	Ticagrelor intercompartmental clearance
V_2	$\text{L} \times \text{kg}^{-1}$	1.8	1.8	1.32, 1.88 ^b	Ticagrelor volume of second compartment
V	$\text{L} \times \text{kg}^{-1}$	0.05	0.05 (not estimated)	–	MEDI2452 (central compartment) volume of distribution. Standard plasma volume.
Cl_f	$\text{L} \times \text{min}^{-1} \times \text{kg}^{-1}$	0.0030	0.0025	0.0024, 0.0026 ^b	MEDI2452 Cl. Initial estimate scaled value from rat ($0.0048 \text{ L} \times \text{min}^{-1} \times \text{kg}^{-1}$) adjusted to 60% to match data.
Cl_{fast}	$\text{L} \times \text{min}^{-1} \times \text{kg}^{-1}$	10	10 (not estimated)	–	Rapid compared to other clearances in the system
σ_{tica}^2	$\text{nM} \times \text{nM}$		0.076	0.064, 0.081 ^b	
σ_{TAM}^2	$\text{nM} \times \text{nM}$		0.080	0.076, 0.087 ^b	
σ_{MEDI}^2	$\text{nM} \times \text{nM}$		0.28	0.26, 0.31 ^b	
$\sigma_{freeTica}^2$	$\text{nM} \times \text{nM}$		0.042	0.039, 0.045 ^b	
$\sigma_{freeTAM}^2$	$\text{nM} \times \text{nM}$		0.060	0.057, 0.069 ^b	

TAM, ticagrelor active metabolite; Tica, ticagrelor.

^aFifth and 95th percentiles obtained from internal data ($n = 38$). ^bFifth and 95th percentiles obtained from bootstrapping. ^c95% confidence interval.⁶

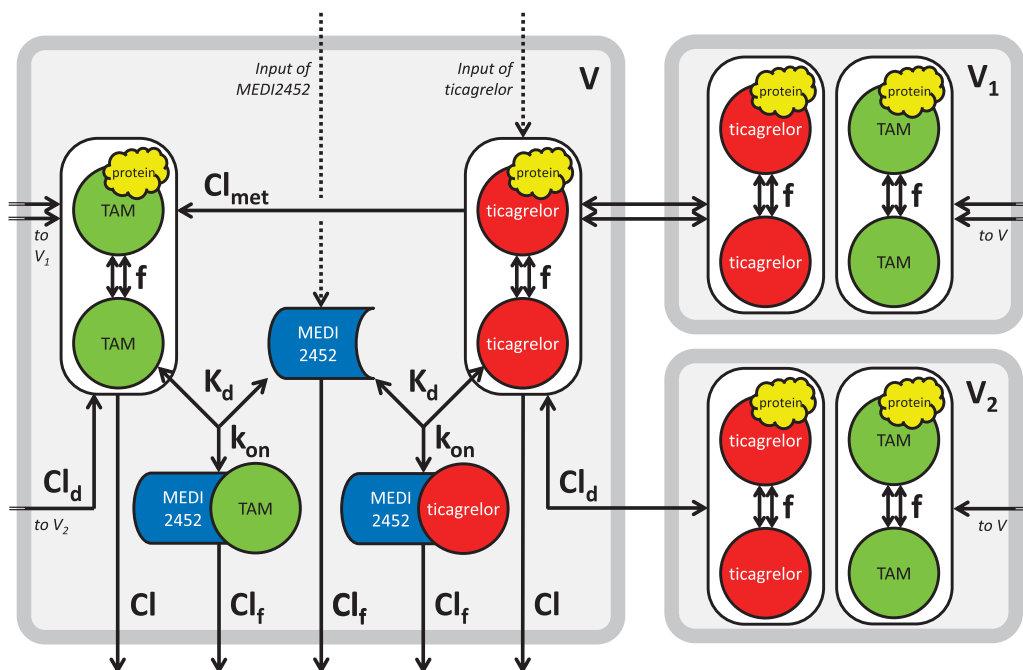


Figure 2 Schematic illustration of the combined ticagrelor-MEDI2452 pharmacokinetic-model. Reactions assumed to equilibrate instantaneously are indicated by double arrows. Input to the system (ticagrelor and MEDI2452) are shown as dashed arrows. The rapid equilibria of free and protein-bound ticagrelor and ticagrelor active metabolite (TAM) are depicted by encapsulated entities. The fractions of free ticagrelor and TAM within these entities are determined by the parameter f . The total contents of free and protein-bound ticagrelor and TAM in the plasma compartment (V) are cleared at the rate Cl , and ticagrelor is additionally being metabolized to TAM at the rate Cl_{met} . The total content of the encapsulated ticagrelor entity may furthermore distribute instantaneously to one peripheral compartment (V_1), and more slowly, with the intercompartmental clearance Cl_d , to another (V_2). Free ticagrelor and TAM in the plasma compartment can reversibly bind to free MEDI2452 with the rate k_{on} , forming complexes with dissociation constant K_d . Both the complexes and free MEDI2452 are cleared at the rate Cl_f .

the absence of ticagrelor was adequately described using a one-compartment model during the timescale of interest. This timescale was dictated by the experiments in which both compounds were administered and occurred over 80 minutes after drug dosing. The parameters of the rat MEDI2452 model were furthermore adjusted based on allometric scaling and *a priori* knowledge of mouse plasma volume to describe the presumed kinetics in the mouse (**Supplementary Text S2**).

A combined ticagrelor-MEDI2452 PK model

A combined ticagrelor-MEDI2452 PK model was hypothesized by integrating the independently derived models for the respective compounds. To this end, assumptions were required with respect to the reconciliation of compartment structures of the two independent models and with respect to certain kinetic matters brought to the fore by the model integration.

Because the central compartment of the independent MEDI2452 model equaled the mouse plasma volume, and because the larger central compartment of the independent ticagrelor and TAM model could be reasonably expected to contain the plasma volume, we assumed the central compartment of the independent ticagrelor and TAM model to be divided into two subcompartments for the hypothesized combined model. A plasma compartment that is identical to the central compartment of independent MEDI2452 model,

with the previously introduced volume V (**Supplementary Text S2**), and a compartment representing tissue rapidly exchanging with plasma, with the new volume V_1 , now representing the remainder of the previous ticagrelor and TAM central compartment. Thus, V accommodates all compounds, whereas V_1 is only for ticagrelor and TAM. The peripheral compartment with volume V_2 of the independent ticagrelor and TAM model (**Supplementary Text S2**) was kept unchanged.

We further assumed that: (I) binding and unbinding of ticagrelor and TAM to plasma protein is fast (i.e., the reaction is considered to reach equilibrium instantaneously); (II) distribution between V and V_1 also is fast in the above sense; (III) the ticagrelor-MEDI2452 complex is cleared at the same rate as MEDI2452; and (IV) the kinetics of TAM is governed by the same principles as ticagrelor (i.e., the equations are structurally equivalent, using the same parameters as for ticagrelor). Assumption (I) is a standard assumption within PK modeling because this equilibrium typically is reached on a timescale of seconds, and it is justified in our case in which the other dynamics occur on a timescale of minutes. Assumption (II) is reasonable because we were not able to improve the separate ticagrelor PK model by adding a third compartment. Assumption (III) is natural if no other information is available and it has been used in similar modeling situations.^{13–15} Regarding assumption (IV), all aspects of TAM kinetics have not been

investigated, but it is known that the affinities of both MEDI2452 and P2Y₁₂ for TAM,⁶ (data on file) are highly similar to the corresponding affinities for ticagrelor.^{6,16} The possibility of target-mediated drug disposition was excluded from the model according to the discussion in **Supplementary Text S2**.

The model is illustrated in **Figure 2**. It is defined by the following equations:

$$\begin{aligned} V \times TicaV(t)' &= -Cl_{fast} \times (TicaV(t) - TicaV_1(t)) \\ &\quad - Cl_d \times (TicaV(t) - TicaV_2(t)) \\ - V \times k_{on} &\left(f \times TicaV(t) \times FabV(t) - K_d \times FabTicaV(t) \right) \\ &\quad - Cl_{met} \times TicaV(t) - Cl \times TicaV(t) + TicaInput(t), \end{aligned} \quad (1)$$

$$V_1 \times TicaV_1(t)' = Cl_{fast} \times (TicaV(t) - TicaV_1(t)), \quad (2)$$

$$V_2 \times TicaV_2(t)' = Cl_d \times (TicaV(t) - TicaV_2(t)), \quad (3)$$

$$\begin{aligned} V \times TamV(t)' &= -Cl_{fast} \times (TamV(t) - TamV_1(t)) \\ &\quad - Cl_d \times (TamV(t) - TamV_2(t)) \\ - V \times k_{on} &\left(f \times TamV(t) \times FabV(t) - K_d \times FabTamV(t) \right) \\ &\quad + Cl_{met} \times TicaV(t) - Cl \times TamV(t), \end{aligned} \quad (4)$$

$$V_1 \times TamV_1(t)' = Cl_{fast} \times (TamV(t) - TamV_1(t)), \quad (5)$$

$$V_2 \times TamV_2(t)' = Cl_d \times (TamV(t) - TamV_2(t)), \quad (6)$$

$$\begin{aligned} V \times FabV(t)' &= - V \times k_{on} \left(f \times TicaV(t) \times FabV(t) - K_d \times FabTicaV(t) \right) \\ &\quad - V \times k_{on} \left(f \times TamV(t) \times FabV(t) - K_d \times FabTamV(t) \right) \\ &\quad - Cl_f \times FabV(t) + FabInput(t), \end{aligned} \quad (7)$$

$$\begin{aligned} V \times FabTicaV(t)' &= V \times k_{on} \left(f \times TicaV(t) \times FabV(t) - K_d \times FabTicaV(t) \right) \\ &\quad - Cl_f \times FabTicaV(t), \end{aligned} \quad (8)$$

$$\begin{aligned} V \times FabTamV(t)' &= V \times k_{on} \left(f \times TamV(t) \times FabV(t) - K_d \times FabTamV(t) \right) \\ &\quad - Cl_f \times FabTamV(t), \end{aligned} \quad (9)$$

where the state variables $TicaV(t)$, $TicaV_1(t)$, $TicaV_2(t)$, $TamV(t)$, $TamV_1(t)$, and $TamV_2(t)$ refer to the time-dependent concentrations of free and protein-bound (not including MEDI2452) ticagrelor and TAM in V , V_1 , and V_2 , respectively, where $FabV(t)$ refers to MEDI2452 concentration in V , and where $FabTicaV(t)$ and $FabTamV(t)$ refer to the ticagrelor-MEDI2452, and TAM-MEDI2452 complexes in V . Values of the parameters, and their justifications, are reported in **Table 1**.

Observation model

The reactions in which ticagrelor and TAM form complexes with MEDI2452 do, in general, never fully reach their equilibria

in the *in vivo* system. This is due to the continuously ongoing clearance and redistribution of the interacting species, which interferes with the processes of reaching the equilibria. When blood samples are collected, however, physiological reactions, like clearances and intercompartmental distribution, are interrupted, and there is sufficient time available for reaching the equilibria before the bioanalysis of the sample content is complete. Because of this, a model of the dynamic process taking place *in vitro* is required in addition to the original model of the *in vivo* system. Such an observation model can mathematically be constructed by setting the values of all clearance parameters to zero, reflecting the *in vitro* conditions of the bioanalysis, and then compute the closed-form analytical solution for the equilibria (**Supplementary Text S2**). The use of the observation model is critical for distinguishing between actual levels of free ticagrelor and TAM, and of measured values (**Supplementary Figure S3**). Specifically, the observed concentrations of free ticagrelor and free TAM are less than the concentrations of free ticagrelor and free TAM in the *in vivo* system. For free levels of MEDI2452, which is present in larger concentrations compared to free ticagrelor and TAM, the difference of using the observation model becomes marginal.

The hypothesized model explains observed data from four separate studies

The model was validated on experimental data from study 1 to 4, comprising different dosing and sampling schedules (**Figure 1**). By a reduction (40%) of the allometrically scaled MEDI2452 clearance (corresponding to scaling rat-mouse with exponent 1 and not 0.75), and without changing any other parameter value, we could reasonably well simulate all the qualitative characteristics of the observed data (**Figure 3**), as well as many of the quantitative characteristics. For studies 1 to 3, the predicted time profiles of plasma levels of total ticagrelor, total TAM, and free MEDI2452 were generally in accordance with data, although there was some underprediction of total ticagrelor and total TAM in the absence of MEDI2452, especially in study 3. For study 4, both model and data displayed increasing levels of total ticagrelor, total TAM, and free MEDI2452, as a function of dose, as well as decreasing levels of free ticagrelor and free TAM as a function of dose. Although the model performed reasonably well for total and free ticagrelor and TAM in study 4, there was a tendency to underpredict free ticagrelor and free TAM and at lower doses there was an overprediction of free MEDI2452.

The validation data were subsequently used to refine the model by reestimation of some of its parameters (**Table 1**). As shown in **Figure 3**, the refined model improved the fit to data in general, including – to us – the particularly important levels of free ticagrelor and free TAM. A residual plot for the refined model is presented in **Supplementary Figure S4**.

Ticagrelor is not likely to be fully recycled

When ticagrelor-bound or TAM-bound MEDI2452 is eliminated in the kidneys, it is currently not known if ticagrelor and TAM are eliminated, recycled, or a combination thereof. Fabs are, however, generally cleared through the kidneys and elimination is faster than for immunoglobulin G (IgG).¹⁷

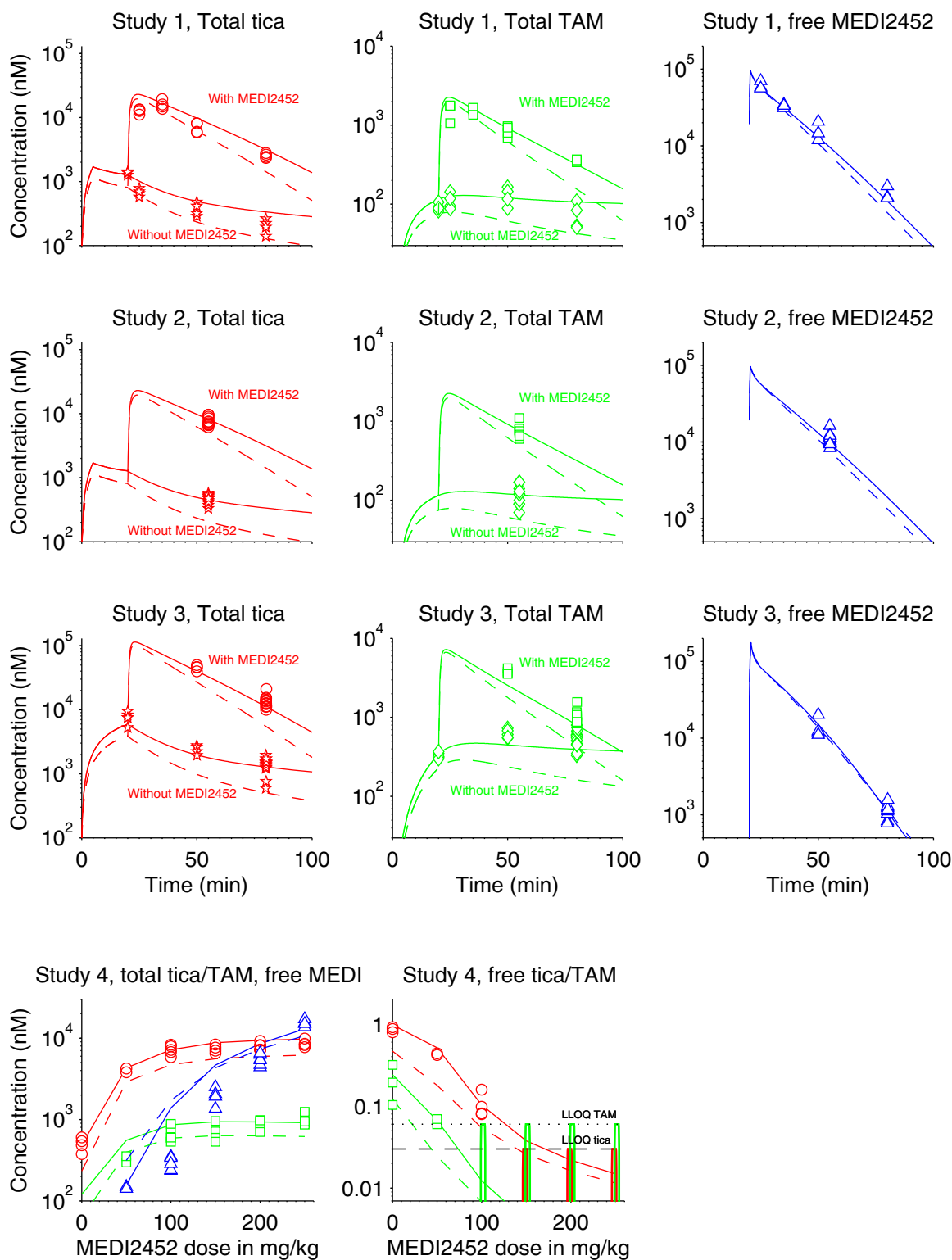


Figure 3 Model validation and refinement. Observed total and free ticagrelor (tica) in plasma are shown as red circles (when MEDI2452 has been coadministered) or red stars (without MEDI2452), observed total and free ticagrelor active metabolite (TAM) in plasma as green squares (with MEDI2452) or green diamonds (without MEDI2452), and observed free MEDI2452 in plasma as blue triangles. Model simulations of ticagrelor, TAM, and MEDI2452 are shown in red, green, and blue lines, respectively. Dashed lines indicate the initially hypothesized model, and solid lines the refined model. LLOQ, lower limit of quantification.

Our main hypothesis (assumption III) has therefore been that both compounds are eliminated intact via the urine as a complex together with MEDI2452, and the model based on this assumption fits data reasonably well. To challenge this assumption we instead assumed that a fraction r of cleared ticagrelor and TAM is recycled. This was implemented in the model by adding the terms $r \times Cl_f \times FabTicaV(t)$ and $r \times Cl_f \times FabTamV(t)$ to the right-hand sides of Eq. (1) and (4), respectively. For the values 0.25, 0.5, and 1 of the recycling fraction r , the previously refined model parameters were then reestimated. The resulting negative log-likelihood values (174, 287, and 613) show that the model becomes increasingly inferior for higher degrees of recycling. These values should also be compared to the model completely lacking recycling, whose negative log-likelihood value is 95 and thereby remains the best model. The same conclusion also follows from inspecting the model simulations in **Figure 4**; whereas the model of total ticagrelor and total TAM are only slightly worsened by the successive increase in the recycled fraction, free levels of ticagrelor and TAM are worse, and free MEDI2452 levels are drastically impaired.

Predicted total ticagrelor plus TAM and free ticagrelor plus TAM in plasma show opposite response after administration of MEDI2452

The refined model was subsequently used to predict the dynamics of both observed and unobserved variables in studies 1 to 4. For these predictions, the effects of both parameter uncertainties and residual variability were taken into account. This was done by Monte Carlo simulations in which parameter values were sampled according to the uncertainties derived from formal parameter estimation or from uncertainties reported in literature. **Figure 5** shows simulations of total ticagrelor plus TAM, free MEDI2452, and free ticagrelor plus TAM in V in response to coadministration of ticagrelor with either MEDI2452 or vehicle. For all designs, total ticagrelor plus TAM and free ticagrelor plus TAM in plasma show opposite response after administration of MEDI2452, with total levels rising while free levels drop. We also note that the levels of free ticagrelor plus TAM after administration of MEDI2452 always remain below the corresponding levels for the vehicle groups during the 100 minutes of the experiments. Importantly, the predictions in **Figure 5** were computed for the *in vivo* levels of free ticagrelor plus TAM (i.e., the observation model was not used). As previously explained, and illustrated in **Supplementary Figure S3**, true *in vivo* levels and measured levels in *ex vivo* samples of ticagrelor and TAM may differ significantly.

The PK model can drive the PD response using a standard turnover model

Inhibition of platelet aggregation stimulated by ADP is a commonly used PD marker for P2Y₁₂ receptor antagonists, both in animals and in the clinic. The predicted levels of free ticagrelor plus TAM were therefore used to drive a simple turnover model describing the dynamics of platelet aggregation, as described in detail in **Supplementary Text S2**. As seen in **Figure 6**, the combined ticagrelor-MEDI2452 PK model extended with a platelet aggregation PD model can describe

experimental data in a quite satisfactory way. A residual plot for the PD model is provided in **Supplementary Figure S5**.

DISCUSSION

Mathematical PK models accounting for the effects of an interfering antidote are scarce in the literature, indicating that this kind of modeling remains largely unexplored. A few existing examples include modeling of so-called inverse targeting strategies, in which antidrug antibodies are administered to reduce systemic drug toxicities.^{13–15,18} There are similarities between our model and the class of target-mediated drug disposition models^{19–21} in the sense that it mechanistically accounts for the buffering interaction of ticagrelor (and TAM) with another molecular species. In our case, the interacting entity is not the drug target, but instead an antidote. Like the target-mediated drug disposition models, which in addition to the interaction itself also includes other necessary aspects of the target dynamics, such as its turnover, our model also includes the parts of the antidote dynamics that are not directly affecting its interaction with ticagrelor (i.e., its distribution and clearance). However, in contrast to our model in which the dynamic aspect of ticagrelor-antidote binding is preserved, target-mediated drug disposition models are frequently simplified according to the rapid-binding assumption.²²

As a step toward validating the model, it was compared to completely fresh data that had not been used for setting up the model. Strictly speaking, models can never be validated but the confidence in a model gradually increases as it successfully predicts new experiments and repeatedly withstands attempts of falsification.²³ Given a minor change in the parameter value for MEDI2452 clearance, the model successfully described the qualitative characteristics of the experimental data of total and free ticagrelor and TAM, and free MEDI2452, in four different studies. Many of the quantitative characteristics were also acceptably well described. Considering the simplicity of allometric scaling it is fully reasonable that a parameter value not derived from mouse data would require a slight final adjustment. By additionally reestimating some of the model parameters, allowing the validation data to inform the inference, an even better description of the data with respect to the quantitative details was possible. Moreover, the successful application of free level predictions to platelet aggregation data further contributes to validating the combined ticagrelor-MEDI2452 PK model. The overall outcome of the model validation and refinement is encouraging and suggests that the principles and assumptions underlying the model are sound and that the model has true predictive capabilities. However, there are still possible improvements to be made, for instance, by considering a full nonlinear mixed effects approach.^{24,25}

A naive analysis of the data may suggest that administration of MEDI2452 is a counterproductive strategy for neutralizing the effects of ticagrelor because it results in a rapid increase by more than an order of magnitude in the total plasma levels of both ticagrelor and TAM. Similar observations of rapidly increasing total levels after antidote administration have been made for colchicine,²⁶

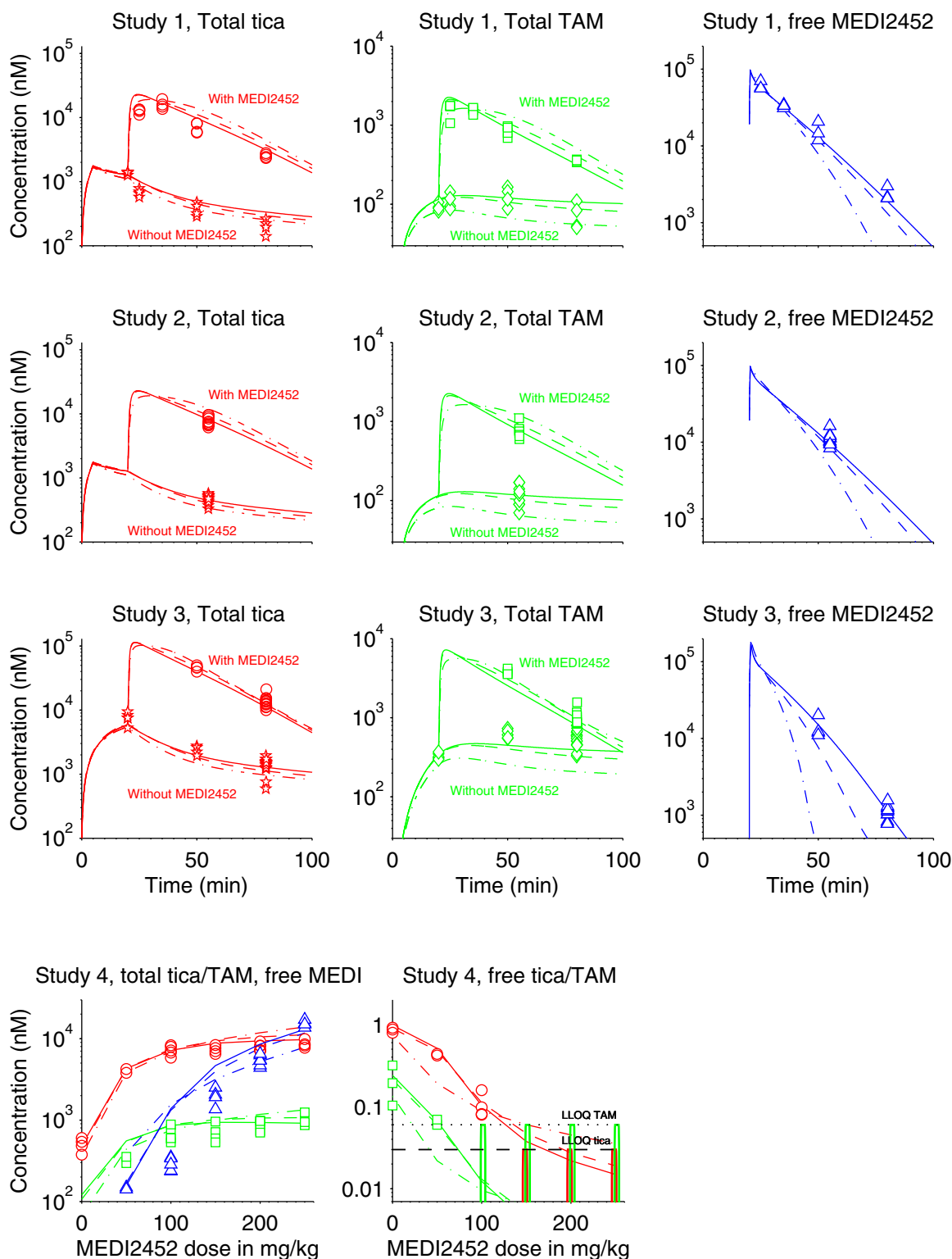


Figure 4 Comparison of alternative models with different degrees of recycling of MEDI2452-bound ticagrelor (tica) and ticagrelor active metabolite (TAM) upon MEDI2452 elimination. Model simulations of 0% of ticagrelor, TAM, and MEDI2452 are shown in red, green, and blue, respectively. Solid lines correspond to model simulations with 0% recycling, dashed lines to 25%, and dashed-dotted lines to 100%. Plotting of observed data follows the same organization as in **Figure 3**. The model's ability to describe the observations decreases as the fraction of recycling increases.

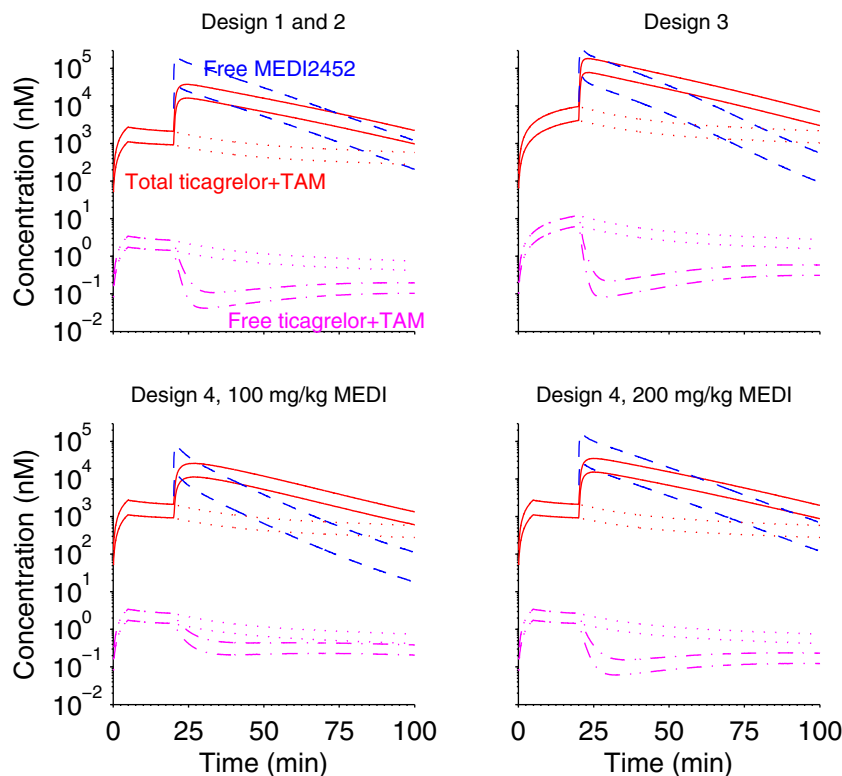


Figure 5 Prediction based on the validated model for studies 1 to 4. Curves represent the simulated 5th and 95th percentiles of the sum of free ticagrelor and free ticagrelor active metabolite (TAM) in plasma (red solid lines), sum of total ticagrelor and TAM in plasma (red solid lines), and free MEDI2452 (MEDI) in plasma (blue dashed line). The dotted lines indicate the scenario with ticagrelor infusion followed by vehicle instead of MEDI2452. The impact of both parameter uncertainty and residual variability is considered for the prediction (**Supplementary Text S2**).

dabigatran,²⁷ and rivaroxaban.¹² However, model simulations show that, despite the large increases in total plasma ticagrelor levels, the free levels in fact display an opposite response after administration of MEDI2452. Reasoning about the structure and parameter values of the model helps to explain the relationship between total and free plasma ticagrelor. Because the volume of distribution for ticagrelor is much larger compared to MEDI2452 (i.e., $V+V_1+V_2 \gg V$), free ticagrelor that is bound by MEDI2452 is rapidly replenished from V_7 , and on a slower timescale also from V_2 . Thus, MEDI2452 is effectively acting like a buffer for ticagrelor in the plasma compartment, causing a substantial accumulation of total ticagrelor in the plasma. A similar explanation can be used for understanding the increase in total TAM. Moreover, if the molar dose of MEDI2452 is comparable to or larger than the total amount of ticagrelor and TAM in all three compartments at the time of dosing, MEDI2452 will bind sufficient ticagrelor and TAM to induce a significant reduction of their free levels in all compartments, including plasma. Although some of the qualitative behaviors of the combined ticagrelor-MEDI2452 PK can be understood from pure reasoning like above, the quantitative details are harder to grasp by intuition because of the nonlinear interaction of ticagrelor and MEDI2452, the delayed distribution of ticagrelor to V_2 , and the metabolism of ticagrelor to TAM, which, in turn, also competes for MEDI2452.

The ability to predict the plasma concentrations of free ticagrelor and free TAM are the key results from the present work. Knowledge about these levels is important because they drive the PD response and therefore also predict the efficacy of MEDI2452. Having access to a trustworthy model is advantageous because it can be used as a complement or an alternative to experimental observations.^{20,21} Although model simulations of the measured free ticagrelor and TAM have been validated, at least to some degree, all simulations of the actual free levels *in vivo* (**Figure 5**) are untested predictions. In fact, these predictions are not only untested but also untestable given the current experimental procedure of measuring free levels of ticagrelor and TAM. Mathematical modeling is therefore a necessity for unraveling the details of the combined ticagrelor-MEDI2452 PK.

The values of the model parameters—both the parameters estimated in the present work and those taken from literature—are uncertain to some degree, and, as a consequence, the model predictions are uncertain too. Providing a measure of uncertainty for the model state variables is often more interesting than the parameter uncertainties, but, unfortunately, also often overlooked. We have showed that, despite the parameter uncertainty, the behavior of the model predictions is relatively well defined. In addition to uncertainties in parameter values, there may be uncertainties with respect to the model structure. It is, for instance, not known what happens to ticagrelor and TAM when ticagrelor-bound

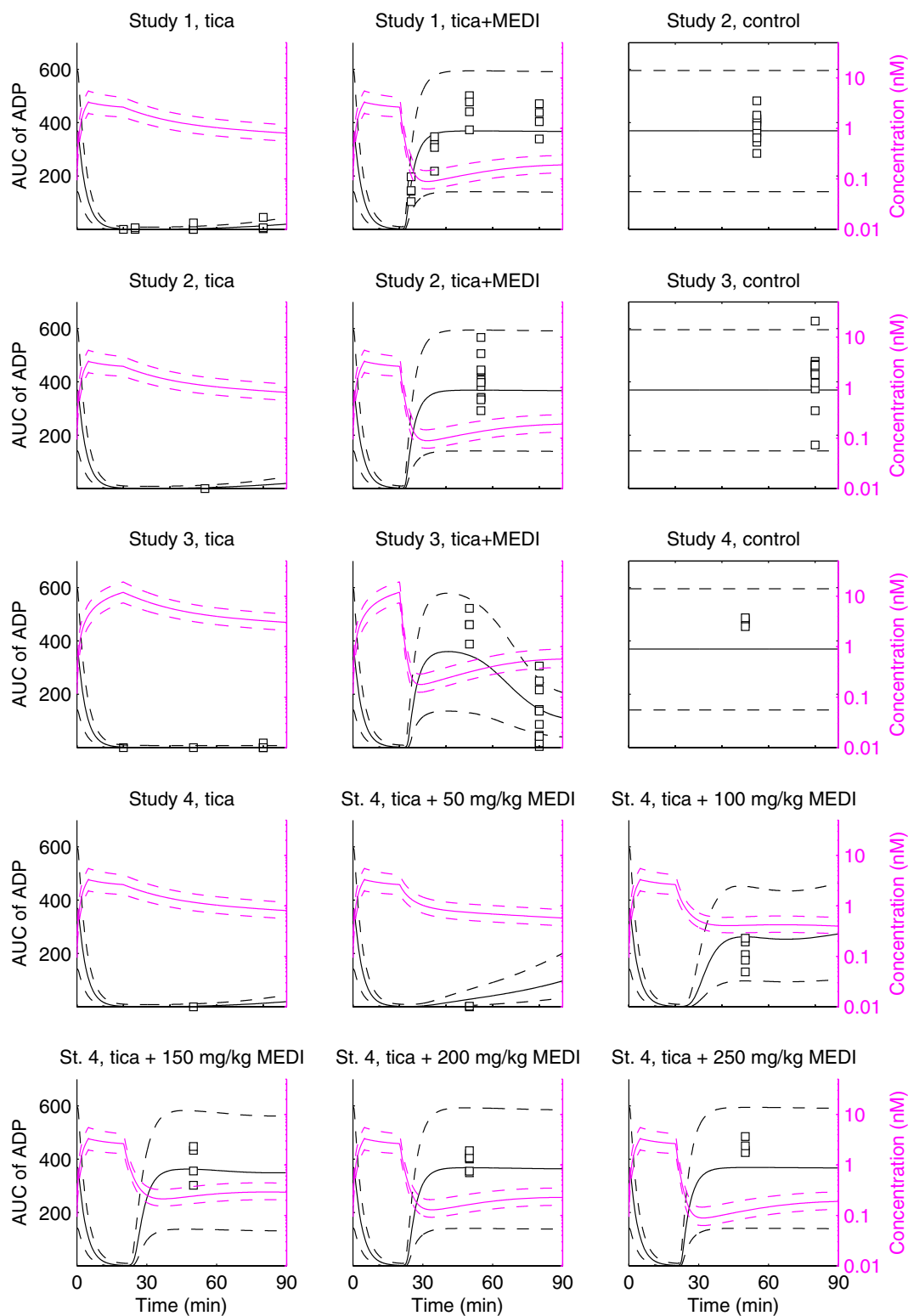


Figure 6 Pharmacokinetic-pharmacodynamic (PK-PD) model performance. The left axis shows simulated (solid black lines) and observed (squares) areas under the curve (AUCs) of ADP-induced platelet aggregation response in whole blood *ex vivo* (arbitrary units). The right axis displays (solid magenta lines) corresponding simulations of the sum of free ticagrelor (tica) and ticagrelor active metabolite (TAM) in plasma (V) which drive the pharmacodynamic effect. The impact of both parameter uncertainty and residual variability is considered in the prediction (**Supplementary Text S2**). Solid curves represent the median and dotted curves represent the simulated 5th and 95th percentiles. St. = Study, MEDI = MEDI2452.

or TAM-bound MEDI2452 is being eliminated, but because of the presumed renal elimination we assumed that no recycling occurs. There are examples of other modeling studies that have considered both full recycling of antibody ligands^{14,15} and partial (25%) recycling of Fab ligands.¹⁴ We showed that model behavior was highly sensitive to introducing a recycling mechanism, and that the corresponding alternative predictions successively became more and more difficult to reconcile with experimental data as the degree of recycling was increased from 0% to 100%. Thus, the modeling supports the view that, in the mouse, when MEDI2452 is eliminated, potential ticagrelor or TAM bound to MEDI2452 is not primarily recycled to the plasma (but eliminated together with MEDI2452), although we would not exclude that a smaller fraction may be. This is an important finding as it constitutes a possible scenario in the extrapolation to humans. The analysis of potential recycling rests on the notion that the clearance of MEDI2452 in the combined PK model represents elimination and not distribution. It was therefore crucial to ensure that the rapid phase of the separate MEDI2452 PK model was due to elimination, before reducing the initial two-compartment model to a one-compartment model (**Supplementary Text S2**).

The proposed model is a good starting point for scaling to model the PK of other species, including humans, and for expansion to a population model. Hence, we anticipate it to be valuable in the future clinical development of MEDI2452.

Conflict of Interest/Disclosure. The authors declared no conflict of interest.

Author Contributions: J.A., S.N., and P.G. wrote the manuscript. J.A., S.P., S.N., and P.G. designed the research. S.P., A.S.S., A.J., S.Maq., S.Mad., and J.G. performed the research. J.A., M.P., S.N., and P.G. analyzed the data.

1. Van Giezen, J.J. *et al.* Ticagrelor binds to human P2Y₁₂ independently from ADP but antagonizes ADP-induced receptor signaling and platelet aggregation. *J. Thromb. Haemost.* **7**, 1556–1565 (2009).
2. Wallentin, L. *et al.* Ticagrelor versus clopidogrel in patients with acute coronary syndromes. *N. Engl. J. Med.* **361**, 1045–1057 (2009).
3. Yusuf, S. *et al.* Effects of clopidogrel in addition to aspirin in patients with acute coronary syndromes without ST-segment elevation. *N. Engl. J. Med.* **345**, 494–502 (2001).
4. Wiviott, S.D. *et al.* Prasugrel versus clopidogrel in patients with acute coronary syndromes. *N. Engl. J. Med.* **357**, 2001–2015 (2007).
5. Bonaca, M.P. *et al.* Long-term use of ticagrelor in patients with prior myocardial infarction. *N. Engl. J. Med.* **372**, 1791–1800 (2015).
6. Buchanan, A. *et al.* Structural and functional characterization of a specific antidote for ticagrelor. *Blood* **125**, 3484–3490 (2015).
7. Dolgin, E. Antidotes progress for new oral clotbusters. *Nat. Biotechnol.* **33**, 117–118 (2015).
8. Schiele, F. *et al.* A specific antidote for dabigatran: functional and structural characterization. *Blood* **121**, 3554–3562 (2013).
9. Glund, S. *et al.* A randomised study in healthy volunteers to investigate the safety, tolerability and pharmacokinetics of idarucizumab, a specific antidote to dabigatran. *Thromb. Haemost.* **113**, 943–951 (2015).
10. Glund, S. *et al.* Safety, tolerability, and efficacy of idarucizumab for the reversal of the anticoagulant effect of dabigatran in healthy male volunteers: a randomised, placebo-controlled, double-blind phase 1 trial. *Lancet* **386**, 680–690 (2015).
11. Pollack, C.V. Jr. *et al.* Idarucizumab for dabigatran reversal. *N. Engl. J. Med.* **373**, 511–520 (2015).
12. Lu, G. *et al.* A specific antidote for reversal of anticoagulation by direct and indirect inhibitors of coagulation factor Xa. *Nat. Med.* **19**, 446–451 (2013).
13. Balthasar, J. & Fung, H.L. Utilization of antidrug antibody fragments for the optimization of intraperitoneal drug therapy: studies using digoxin as a model drug. *J. Pharmacol. Exp. Ther.* **268**, 734–739 (1994).
14. Lobo, E.D., Soda, D.M. & Balthasar, J.P. Application of pharmacokinetic-pharmacodynamic modeling to predict the kinetic and dynamic effects of anti-methotrexate antibodies in mice. *J. Pharm. Sci.* **92**, 1665–1676 (2003).
15. Shah, D.K. & Balthasar, J.P. PK/TD modeling for prediction of the effects of 8C2, an anti-topotecan mAb, on topotecan-induced toxicity in mice. *Int. J. Pharm.* **465**, 228–238 (2014).
16. Springthorpe, B. *et al.* From ATP to AZD6140: the discovery of an orally active reversible P2Y₁₂ receptor antagonist for the prevention of thrombosis. *Bioorg. Med. Chem. Lett.* **17**, 6013–6018 (2007).
17. King, D.J. *Applications and Engineering of Monoclonal Antibodies* (Taylor & Francis Ltd, London, 1988).
18. Balthasar, J.P. & Fung, H.L. Inverse targeting of peritoneal tumors: selective alteration of the disposition of methotrexate through the use of anti-methotrexate antibodies and antibody fragments. *J. Pharm. Sci.* **85**, 1035–1043 (1996).
19. Mager, D.E. & Jusko, W.J. General pharmacokinetic model for drugs exhibiting target-mediated drug disposition. *J. Pharmacokinet. Pharmacodyn.* **28**, 507–532 (2001).
20. Xiao, J.J. *et al.* Pharmacokinetics of anti-hepcidin monoclonal antibody Ab 12B9m and hepcidin in cynomolgus monkeys. *AAPS J.* **12**, 646–657 (2010).
21. Tang, C. & Prueksaranont, T. Theoretical analysis of interplay of therapeutic protein drug and circulating soluble target: temporal profiles of 'free' and 'total' drug and target. *Pharm. Res.* **28**, 2447–2457 (2011).
22. Marathe, A., Krzyzanski, W. & Mager, D.E. Numerical validation and properties of a rapid binding approximation of a target-mediated drug disposition pharmacokinetic model. *J. Pharmacokinet. Pharmacodyn.* **36**, 199–219 (2009).
23. Almquist, J., Cvijovic, M., Hatzimanikatis, V., Nielsen, J. & Jirstrand, M. Kinetic models in industrial biotechnology – improving cell factory performance. *Metab. Eng.* **24**, 38–60 (2014).
24. Bonate, P. *Pharmacokinetic-Pharmacodynamic Modeling and Simulation* (Springer, New York, 2006).
25. Almquist, J., Leander, J. & Jirstrand, M. Using sensitivity equations for computing gradients of the FOCE and FOCEI approximations to the population likelihood. *J. Pharmacokinet. Pharmacodyn.* **42**, 191–209 (2015).
26. Sabouraud, A.E., Urtizberea, M., Cano, N.J., Grandgeorge, M., Rouzioux, J.M. & Schermann, J.M. Colchicine-specific Fab fragments alter colchicine disposition in rabbits. *J. Pharmacol. Exp. Ther.* **260**, 1214–1219 (1992).
27. Almquist, J., Litzemberger, T., Gan, G., Coble, K. & Schurer, J. In vitro characterization, pharmacokinetics and reversal of supratherapeutic doses of dabigatran-induced bleeding in rats by a specific antibody fragment antidote to dabigatran. 54th ASH Annual Meeting and Exposition, Atlanta, GA, 8–11 December 2012. Abstract 3418.

© 2016 The Authors CPT: Pharmacometrics & Systems Pharmacology published by Wiley Periodicals, Inc. on behalf of American Society for Clinical Pharmacology and Therapeutics. This is an open access article under the terms of the Creative Commons Attribution-NonCommercial License, which permits use, distribution and reproduction in any medium, provided the original work is properly cited and is not used for commercial purposes.

Supplementary information accompanies this paper on the CPT: Pharmacometrics & Systems Pharmacology website (<http://www.wileyonlinelibrary.com/psp4>)